



Article

Optimized PID control for automated blood pressure management in post-operative care

Jegatheesh Anbazhagan^{1*}, Siddheswar Kar², Krishna Prakash Arunachalam³,
Aravinda Koithyar⁴

¹Department of Electronics and Communication Engineering, Infant Jesus College of Engineering, Tuticorin, India

²Department of Electrical Engineering, Medicaps University, Indore, M.P, India

³Departamento de Ciencias de la Construcción, Facultad de Ciencias de la Construcción Ordenamiento Territorial, Universidad Tecnológica Metropolitana, Santiago, Chile

⁴Department of Electronics and Communication Engineering, New Horizon College of Engineering, Bengaluru, India

ARTICLE INFO

Article history:

Received 30 March 2025

Received in revised form

12 May 2025

Accepted 25 May 2025

Keywords:

Blood pressure, Sodium nitroprusside, Prairie dog optimization, Proportional-integral-derivative controller, Infusion pump

*Corresponding author

Email address:

jegatheeha@gmail.com

DOI: 10.55670/fpll.futech.4.3.2

ABSTRACT

Maintaining optimal Blood Pressure (BP) is vital, as abnormal BP levels pose substantial challenges to patient recovery in post-operative care. The manual administration of Sodium Nitroprusside (SNP) is a common approach to lower BP by relaxing peripheral vascular smooth muscles. Nevertheless, because of the inconsistency in drug sensitivity between patients, manual dosing is inaccurate and labour-intensive as it necessitates continuous expert monitoring. Therefore, this research adapts a control method to regulate BP in post-operative patients with hypertension. The Prairie Dog Optimization-based Proportional-Integral-Derivative (PDO-PID) controller adapts in real-time to the particular physiological responses of the patients, assuring precise and individualized SNP dosing. According to simulation results, the controller effectively controls BP levels over an extended time, generating an execution time of 63.613s and a reduced settling time of 1.05s. Corresponding SNP infusion levels are also effectively regulated, which is significantly smaller than the previous control approaches.

1. Introduction

Local Personalized hemodynamic management in the Intensive Care Unit (ICU) and Operating Room (OR) requires real-time cardiovascular system monitoring. Severe surgical organ failure results from poorly treated perioperative hypotension (low BP) and hypertension (high BP) [1]. According to estimates, elevated BP is the primary risk factor for 10.4 million deaths annually, and the number is continually growing. Acute blood pressure increases are frequently linked to major outcomes that need immediate medical attention [2, 3]. On the other hand, poor blood pressure control might endanger brain perfusion, which causes ischemia, infarction, and even neurological impairments. Optimizing blood pressure regulation before and after awake craniotomy is consequently a challenge in order to reduce the danger of bleeding as well as the possibility of neurological impairments. Continuous blood pressure monitoring is necessary, as certain patients require temporary anti-hypertensive medications following glioma excision via craniotomy, and invasive blood pressure

monitoring is often limited to intermediate or critical care units [4-6]. Even with the introduction of numerous antihypertensive medications in recent decades and the identification of numerous traditional risk factors for hypertension, blood pressure (BP) management in modern society remains suboptimal, with one-fourth of hypertension sufferers failing to meet optimal BP targets [7, 8]. It has been demonstrated that appropriate blood pressure management considerably lowers the cardiovascular morbidity and all-cause mortality linked to hypertension. In order to successfully prevent and treat hypertension, blood pressure needs to be checked on a normal and reliable basis [9-11]. One of the effective drugs to reduce Mean Arterial Blood Pressure (MABP) is SNP, an anti-hypertension vasodilator. Since patients respond differently to this pressure-controlling medication and the regulated release of the drug over an extended period of time, healthcare staff's manual control of MABP using SNP is frequently demanding, exhausting, and of low quality [12,13].

Abbreviation

ABC	Artificial bee colony
ACO	Ant Colony Optimization
BP	Blood Pressure
DS	digging strength
GA	Genetic Algorithm
GWO	Grey Wolf Optimizer
IAE	Integral Absolute Error
ICU	Intensive Care Unit
ISE	Integral Squared Error
ITAE	Integral Time Absolute Error
MAP	Mean Arterial Pressure
MABP	Mean Arterial Blood Pressure
MPC	Model Predictive Control
MSE	Mean Squared Error
OF	objective function
OR	Operating Room
PID	Proportional-Integral-Derivative
PDO	Prairie Dog Optimization
PSO	Particle Swarm Optimization
SNP	Sodium Nitroprusside
SSA	Salp Swarm Algorithm

Therefore, holding MAP within the ideal range is difficult for any patient receiving post-surgical drug infusion, such as SNP. In this situation, the medical practitioner uses manual control to preserve MAP at the proper level in a traditional and straightforward manner [14,15]. Predictive controllers and intelligent techniques work together to control systems with few inputs and outputs in a very effective and potent manner. Actually, the controller is aware of the limitations on both input and output, and it never generates an input signal that deviates from them. In general, controllers aim to regulate the quantity of medication administered to the body, which in turn regulates BP and lessens surgical and post-operative problems [16]. A multi-model predictive controller that uses many models to properly forecast blood pressure behavior is developed in [17] to handle variances in patient situations. However, using more than one model adds to the computing effort, which makes it difficult for real-time applications. Therefore, this paper develops a PID controller for automatic BP regulation. To enhance the performance of a developed PID controller, an optimization algorithm is exploited. Particle Swarm Optimization (PSO) is represented in [18], minimizes a cost function that is determined by the system response and control objective. This improves control performance by enabling more effective and efficient tuning of the controller parameters. However, the final solution is impacted by the starting population's quality, and inaccurate initial estimations result in less-than-ideal outcomes or longer convergence times. By adjusting the controller's parameters, a Genetic algorithm is developed in [19] to enhance management of blood pressure performance. Suboptimal PID parameters result from its convergence to local optima rather than the global optimum. A PID controller is used in [20] with an Artificial Bee Colony (ABC) algorithm that improves performance. Nevertheless, implementing an ACO-based PID controller is more complex than other methods. As a result, this research proposes a PDO-based PID controller for regulating the BP. The main objectives of this research are:

- Implementing the PID controller for regulating the blood pressure by adjusting medication dosages based on real-time BP interpretations.
- Incorporating the Prairie Dog Optimization for tuning the parameters of the PID controller.

2. Proposed methodology

Figure 1 depicts the BP management system with a PID controller, which has found extensive application in process control. The BP measurement sensor initially measures the patient's BP level. Then, the error generator block outputs the error signal between the measured and desired BP level.

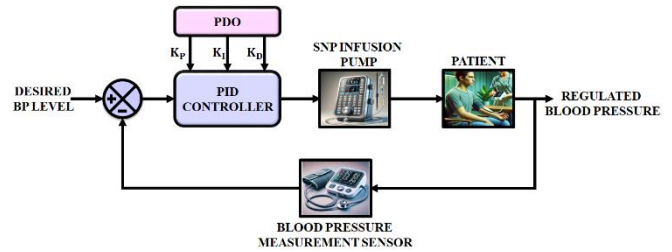


Figure 1. Block diagram of BP management system

This error signal is given to the PID controller, and its parameters are tuned by the PDO algorithm. The PID controller sends an appropriate control signal for the correct administration of the medicine into the injection pump according to the error between the set-point and the patient's measured BP level. Subsequently, the proper amount of SNP is given to the patient, and this process is repeated until the desired BP level is reached.

2.1 Blood pressure model

Cardiac output, vascular resistance, and central venous BP all contribute to blood pressure, which is actually the average BP throughout a heart period. Maintaining MAP management is crucial for lowering hypertension disorders and preventing acute, life-threatening illnesses like stroke. MAP is more precise than the metabolic syndrome predicted by systolic, diastolic, and pulse pressure in older adults with hypertension. Now, the hypoxia-ischaemic brain damage is the leading cause of death in heart attacks. If the MAP is better than the automatic adjustment's threshold, it results in excessive strain, which worsens brain injury and increases brain oedema. Conversely, if the MAP is under the automatic adjustment threshold, it induces further ischemia and brain damage. For these individuals to survive, blood pressure needs to be maintained within an ideal range by utilizing the link between blood pressure and oxygen saturation in the brain tissue. It is often used in general surgeries, hypotensive anaesthesia (anaesthesia by reducing BP) reduces intraoperative bleeding and necessitates postoperative blood transfusions. However, to control important physiological parameters, including awareness, heart rate, MAP, and breathing rate, this anaesthesia necessitates several medication injections. This control system's goal is to lower the patient's MAP by modifying the nitroprusside and medication dosage. This section provides the MAP model for controlling the patient's desired MAP through the infusion of SNP medicine. Figure 2 shows the general structure of the MAP model. The implemented model illustrates the relationship between the SNP medication infusion volumes and the MAP fluctuation for drug administration.

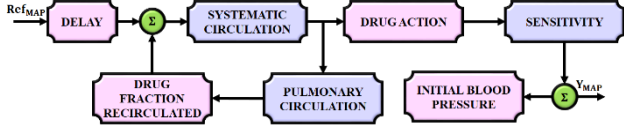


Figure 2. MAP system

The dynamic system is:

$$G_p = \frac{Y_p(s)}{I_p(s)} = \frac{[S_p(1+L_{p3}s)e^{-(\theta_p)s}]}{[(1+L_{p3}s)(1+L_{p2}s)-\delta_p](1+L_{p1}s)} \quad (1)$$

In the dynamic model, I_p represents the rate at which the drug is given, whereas $Y_p(s)$ represents the variations in blood pressure brought on by the SNP drug's infusion. The rate of drug absorption into the patient's system is determined by the drug infusion time constants L_{p1} , L_{p2} and L_{p3} . A fraction of the recirculated SNP drug is indicated by the parameter δ_p , whilst the time interval between the drug infusion and its impact on blood pressure is denoted by θ_p . Finally, S_p shows that the patient's sensitivity to the medication affects their blood pressure. The MAP model is indicated by:

$$MAP_p(t) = Y_p(t) + I_{bp}(0) \quad (2)$$

Where the starting blood pressure is $I_{bp}(0)$. This research's primary objective is to carefully give the drug SNP in order to manage MAP.

2.2 PDO optimized PID controller

To attain optimization, the PDO algorithm simulates the actions of 4 Prairie Dogs (PDs). The burrow-building and eating behaviors of the PDs are exploited to investigate the optimization problem domain. A plentiful supply of food serves as the basis for the PDs' tunnels. They look for alternative food sources or solutions throughout the colony or problem space as the current one runs out. Every time they find a new food source, they dig new tunnels around it. Two distinct warning sounds are exploited to elicit the PDs' unique responses. Anything from the occurrence of predators to the accessibility of food needs to be inferred from the sounds made by PDs. Due to their outstanding communication abilities, the PD can protect themselves from predators and meet their nutritional needs. These two distinct behaviors cause the PDs to congregate in a specific location when the PDO is implemented. From there, exploitation is done to detect better solutions.

2.2.1 Initialization

Similar to other population-based techniques, PDO starts the PDs' positions arbitrarily. The search agents are populations of PDs, and each PD is denoted by a vector in d-dimensional space. Each PD in a coterie belongs to one of the n coterie's. Each Coterie's (CT) location within a colony is,

$$CT = \begin{bmatrix} CT_{1,1} & CT_{1,2} & \dots & CT_{1,d-1} & CT_{1,d} \\ CT_{2,1} & CT_{2,2} & \dots & CT_{2,d-1} & CT_{2,d} \\ \vdots & \vdots & & CT_{i,j} & \vdots \\ CT_{m,1} & CT_{m,2} & \dots & CT_{m,d-1} & CT_{m,d} \end{bmatrix} \quad (3)$$

Where $CT_{i,j}$ is the j^{th} dimension of i^{th} coterie. Each prairie dog's place within a coterie is represented by:

$$PD = \begin{bmatrix} PD_{1,1} & PD_{1,2} & \dots & PD_{1,d-1} & PD_{1,d} \\ PD_{2,1} & PD_{2,2} & \dots & PD_{2,d-1} & PD_{2,d} \\ \vdots & \vdots & & PD_{i,j} & \vdots \\ PD_{n,1} & PD_{n,2} & \dots & PD_{n,d-1} & PD_{n,d} \end{bmatrix} \quad (4)$$

Where $PD_{i,j}$ is the i^{th} prairie dog in a coterie's j^{th} dimension. Based on the expressions given below, a uniform distribution is exploited to distribute each PD and CT site.

$$CT_{i,j} = U(0,1) * (UB_j - LB_j) + LB_j \quad (5)$$

$$PD_{i,j} = U(0,1) * (ub_j - lb_j) + lb_j \quad (6)$$

Where $U(0,1)$ is a uniformly distributed random number among 0 and 1, $ub_j = \frac{UB_j}{m}$, $lb_j = \frac{LB_j}{m}$. The upper and lower bounds of the optimization problem's j^{th} dimensions are denoted by UB_j and LB_j respectively. The flowchart of the PDO algorithm is illustrated in Figure 3.

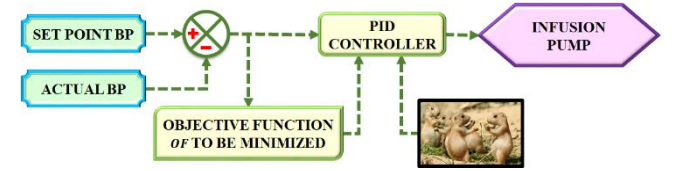


Figure 3. Schematic diagram of PDO-PID controller

2.2.2 Fitness Function Evaluation

After receiving the solution vector, the fitness function estimates the fitness function value for the location of each PD. The obtained values are,

$$f(PD) = \begin{bmatrix} f_1([PD_{1,1} & PD_{1,2} & \dots & PD_{1,d-1} & PD_{1,d}]) \\ f_2([PD_{2,1} & PD_{2,2} & \dots & PD_{2,d-1} & PD_{2,d}]) \\ \vdots & \vdots & & \vdots & \vdots \\ f_n([PD_{n,1} & PD_{n,2} & \dots & PD_{n,d-1} & PD_{n,d}]) \end{bmatrix} \quad (7)$$

The lowest fitness value is the best approach to the specified minimization issue. The fitness function values are preserved in a sorted array. The next three are assumed along with the optimum value for generating burrows that aid them in avoiding predators.

2.2.3 Exploration

A plentiful supply of food helps as the basis for PDs' tunnels. They look for alternative food sources or solutions throughout the colony or problem space as the current one runs out. Every time they find a new food source, they dig new tunnels around it. The burrows are vital for protecting the habitat from predators. Every PD resides in a colony, and each colony is separated into coterie's with different colonial boundaries. Within their limits, the many coterie's forage and dig burrows together only when a predator exists. PDO chooses between exploration and exploitation according to 4 factors. The 4 phases of the highest number of repetitions include exploration and exploitation. Both of these exploratory methods rely on,

$$iter < \frac{Max_{iter}}{4} \text{ and } \frac{Max_{iter}}{4} \leq iter < \frac{Max_{iter}}{2} \quad (8)$$

The two strategies for exploitation are based on:

$$\frac{Max_{iter}}{2} \leq iter \leq 3 \frac{Max_{iter}}{4} \text{ and } 3 \frac{Max_{iter}}{4} \leq iter \leq Max_{iter} \quad (9)$$

The first strategy of coterie through the exploration phase is to have members search the ward for new food sources (Figure 4). The PDs' movements during their meal seeking are best captured by the Levy flight motion. This movement successfully examines a range of places despite preventing a comprehensive search of a specific location due to its characteristic large hops. To notify other people that food sources are found, they make distinctive sounds. In the algorithm's exploration phase, foraging position updating is provided by:

$$PD_{i+1} = \frac{G_{Besti,j} - eCBest_{i,j} \times \rho - CPD_{i,j} \times Levy(n) \forall iter < \frac{Max_{iter}}{4}}{4} \quad (10)$$

$$PD_{i+1,j+1} = \frac{G_{Besti,j} \times rPD \times DS \times Levy(n) \forall \frac{Max_{iter}}{4} \leq iter < \frac{Max_{iter}}{2}}{2} \quad (11)$$

Where $G_{Besti,j}$ denotes the best solution presently available worldwide, and $eCBest_{i,j}$ assesses the consequences of the most effective solution presently acquired worldwide. $CPD_{i,j}$ represents the randomized cumulative effect of all PDs, ρ indicates the experiment's customized food supply alert set at 0.1 kHz, and rPD indicates the position of a random solution. The coterie's digging strength, denoted by DS , which has a random value, is determined by the quality of the food source. The Levy distribution, $Levy(n)$ is well known for promoting more effective and superior problem search space exploration.

$$eCBest_{i,j} = G_{Besti,j} \times \Delta + \frac{PD_{i,j} \times mean(PD_{n,m})}{G_{Besti,j} \times (UB_j - LB_j) + \Delta} \quad (12)$$

$$CPD_{i,j} = \frac{G_{Besti,j} - rPD_{i,j}}{G_{Besti,j} + \Delta} \quad (13)$$

$$DS = 1.5 \times r \times \left(1 - \frac{iter}{Max_{iter}}\right)^{\left(2 \frac{iter}{Max_{iter}}\right)} \quad (14)$$

Where r introduces the stochastic property to validate exploration and takes the value of either 1 or -1 depending on the present iteration, and Δ denotes a small number that indicates discrepancies that arise among the PDs. Max_{iter} is the maximum number of iterations, and $iter$ is the present iteration. To guarantee exploration, the r adds the stochastic property. Depending on the iteration, it takes the value of 1 or -1.

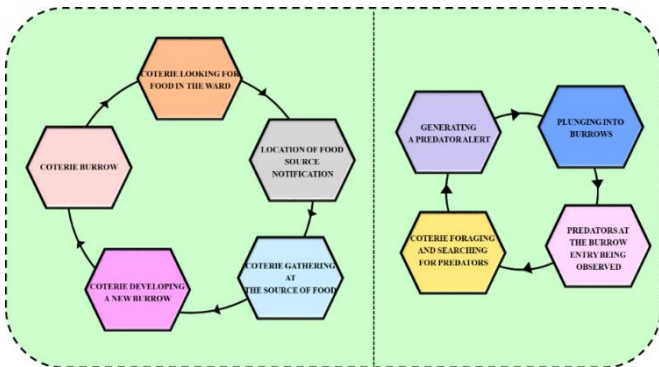


Figure 4. Exploration and exploitation strategy

2.2.4 Exploitation

The PDO capitalizes on PDs' varying responses to two distinct alarms or communication noises. Anything from the presence of predators to the availability of food is inferred from the sounds made by PDs. Because of their outstanding communication abilities, the PDs are able to protect themselves from predators and meet their nutritional needs. Furthermore, only PDs near the bird's path hide, with the others staying in their burrows to observe if the transmission indicates a hawk as the predator. The PDs congregate in one position due to these two distinct behaviors, or in the case of PDO implementation, a potential site where further search is conducted to uncover better or almost ideal solutions. The exploitation processes used by PDO are intended to thoroughly search the potential areas discovered during the exploration stage, as seen in Figure 3. The PDO alternates between these two tactics under the conditions,

$$\frac{Max_{iter}}{2} \leq iter \leq 3 \frac{Max_{iter}}{4} \text{ and } 3 \frac{Max_{iter}}{4} \leq iter \leq Max_{iter} \quad (15)$$

$$PD_{i+1,j+1} = \frac{G_{Besti,j} - eCBest_{i,j} \times \varepsilon - CPD_{i,j} \times rand \forall \frac{Max_{iter}}{2} \leq iter \leq 3 \frac{Max_{iter}}{4}}{2} \quad (16)$$

$$PD_{i+1,j+1} = \frac{G_{Besti,j} \times PE \times rand \forall 3 \frac{Max_{iter}}{4} \leq iter < Max_{iter}}{4} \quad (17)$$

Figure 5 represents the flowchart of the PDO algorithm. Whereas $G_{Besti,j}$ is the most successful worldwide solution to date, $eCBest_{i,j}$ examines the effects of the most recent finest solution. The predator effect is represented by PE , $rand$ is a random integer between 0 and 1, $CPD_{i,j}$ is the combined influence of all PD in the colony, and ε is a minor value that indicates the quality of the food that is available.

$$PE = 1.5 \times \left(1 - \frac{iter}{Max_{iter}}\right)^{\left(2 \frac{iter}{Max_{iter}}\right)} \quad (18)$$

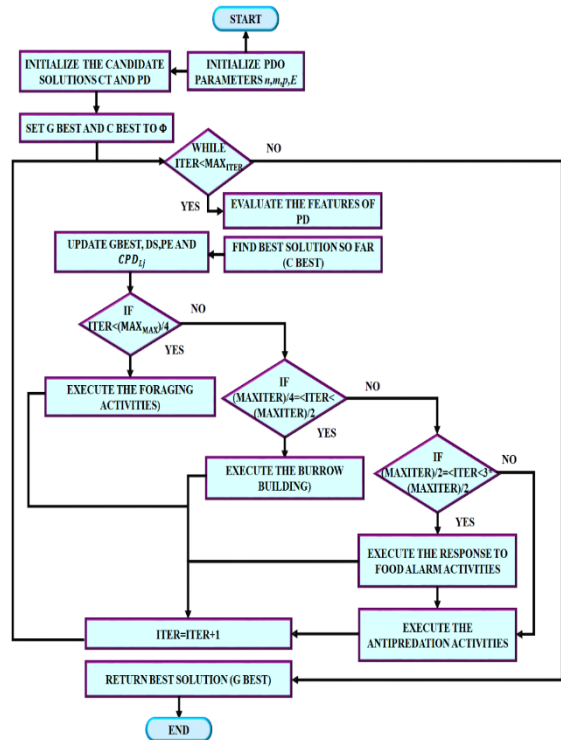


Figure 5. Flowchart of the PDO algorithm

2.2.5 Implementation of PDO-based PID controller

The PDO approach is used in this study to get the best possible blood pressure control. The PDO technique is used to calculate the gain values of the optimal PID parameters. The objective functions are minimized using the Integral Time Absolute Error (ITAE) standard. The objective function is:

$$OF = \int_0^t ((E_r(t))^2 dt) \tag{19}$$

BP management involves maintaining a patient's BP within desired levels by continuously monitoring and regulating the output of a pump. The expression for the PID controller is,

$$u(t) = K_p e(t) + K_i \int_0^t e(t) dt + K_d \frac{de(t)}{dt} \tag{20}$$

Where the error signal is represented by $e(t) = r(t) - y(t)$, control signal is indicated by $u(t)$ and proportional, integral, and derivative gains are denoted by K_p, K_i and K_d . This method assures optimal BP control by integrating the PDO algorithm's ability to balance exploration and exploitation for tuning the PID parameters. Figure 3 depicts the schematic diagram of PDO-PID controller.

2.3 Infusion pump

A basic infusion pump is permitted if the input voltage adjustment at the pump equals the variation in the infusion rate at the output.

$$\dot{u}(t) = v(t) \tag{21}$$

The pump's transfer function is:

$$G_b(S) = \frac{U(S)}{V(S)} = \frac{1}{s} \tag{22}$$

From the perspective of input/output, the infusion pump has an impulse response $h(t) = 1$ for $t \geq 0$.

2.4 Patient

Under the influence of SNP, the patient's MAP is denoted by:

$$MAP(t) = P_o(t) - \Delta P(t) + v(t) \tag{23}$$

Where $v(t)$ is a stochastic background noise, $P(t)$ is the pressure differential because of the infusion of SNP, and P_o is the initial BP, also known as the background pressure. P_o is taken as constant in this paper. The relationship between the change in BP, $\Delta P(s)$ and the drug infusion rate, $I(s)$ is described by the following continuous-time deterministic model:

$$\Delta P(S) = \frac{K e^{-T_i s} (1 + \alpha e^{-T_c s})}{1 + \tau_s} I(S) \tag{24}$$

Where τ a time constant, T_i is the initial transport delay, T_c is the recirculation time delay, α is the recirculation constant, and K is the sensitivity of the drug. The relevant discrete-time deterministic model is,

$$\Delta P(t) = \frac{q^{-d} (b_o + b_m q^{-m})}{1 - a_1 q^{-1}} I(t); b_o > 0 \tag{25}$$

Parameters b_o, b_m, a_1, d and m are taken from the sampled form of the continuous-time model, where q^{-1} represents a unit delay operator. Table 1 lists a range of typical values for the model's parameters for various patients.

The parameters $K, \alpha,$ and τ change during the infusion process, time delays for a particular patient are unknown but are presumed to be consistent over an extended period of time. The following model is used in this work, which assumes that the parameters change exponentially.

Table 1. Values for the model's parameters

Parameters	Maximum	Nominal	Minimum
$T_c(s)$	75	45	30
$T_i(s)$	60	40	20
$\tau(s)$	60	40	20
α	0.4	0.1	0
K	9	1	0.25

$$par(k) = par(0) (2 - e^{-k/\gamma}) \tag{26}$$

Where γ is the change in the time constant and $par(t)$ is the parameter of the continuous-time model for increasing and decreasing the parameter value. As a result, the controller is able to manage time-varying parameters and initially unknown time delays when it is adjusted for a specific patient.

3. Results and discussion

In this section, a dynamics model of MAP is chosen and executed as a controlled system in a simulated environment in order to assess the performance of developed control architecture managed the medicine infusion SNP rate to regulate MAP. The comparison of developed research with conventional approaches for BP management is also included in this section.

The open-loop system's unit step response for the BP management system is displayed in Figure 6. It shows how the system reacts without any feedback control when subjected to a unit step input. The response reveals a slow rise in output, with a significant delay and extended settling time, indicating poor dynamic performance and a lack of regulation in controlling BP.

Figure 7 illustrates the system response to the intended output. The patient's BP is 40 mmHg at the first appointment. Following the intended output, the system response immediately returns blood pressure to normal. It compares the MBP with the reference signal over time. The graph demonstrates that the PDO-PID controller successfully tracks varying reference BP levels with minimal overshoot and rapid settling, even during step changes. This indicates that the proposed controller is capable of maintaining BP within the desired ranges effectively and adaptively, ensuring precise and responsive regulation suitable for post-operative hypertension management.

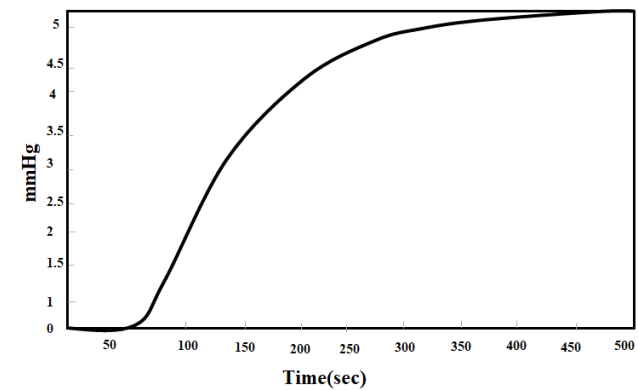


Figure 6. Step response

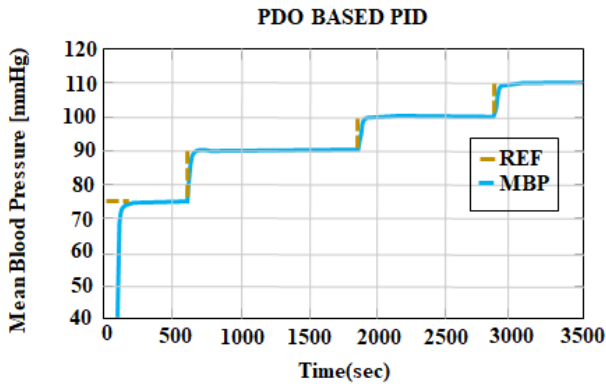


Figure 7. Output response

The impact of the prediction horizon (P) on the response of the system is represented in Figure 8. The signal gets laxer and has an inferior jump than lesser values as the horizon grows, but the computational volume also increases. However, this increase slows down the system. The system speed increases as the prediction horizon lowers, while the quantity of jumps grows in the other direction. Figure 9(A) denotes the output response for the PDO-based PID controller. It compares the MBP with disturbance and the reference signal over varying time. In addition to the heartbeat, injection device, percentage of injection substance, and neurological system, the disturbance is assumed to be sinusoidal. This disturbance has an amplitude of 10. The influence of drug-induced disturbance has been abolished, as seen in Figure 9 (B).

Figures 10 and 11 display the output and control signal of the developed control system. Figure 10 shows the system output stabilizing around 1.2 mmHg shortly after the 75-second mark, maintaining steady performance with negligible fluctuations, which reflects the controller's rapid settling and robust stability.

Figure 11 illustrates the SNP drug infusion rate used to achieve this control. Initially, the infusion rate exhibits some oscillations as the controller adapts to the system dynamics, but it quickly stabilizes to a constant rate of around 0.6 mL/h, indicating efficient and consistent drug administration with minimal overshoot. The PDO-PID controller satisfies the constraint of the drug infusion rate limitation. Both the output and control signal are varied initially and maintained a steady value.

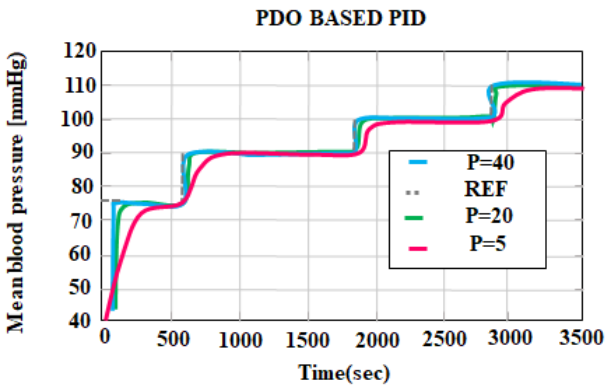
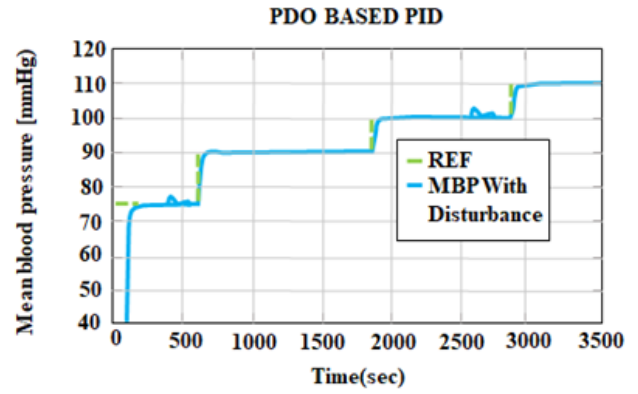
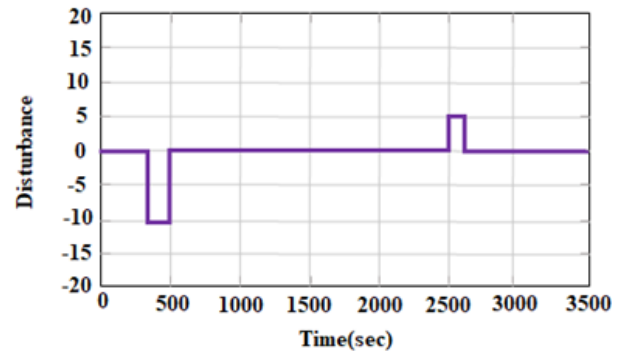


Figure 8. MAP for diverse values of P



(a)



(b)

Figure 9. (a) Output response for PDO-based PID (b) Impact of drug disturbance on the patient

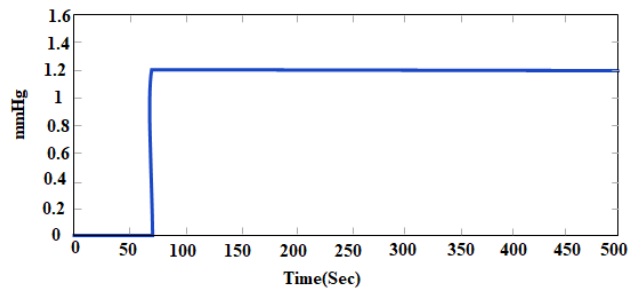


Figure 10. Output response with PDO-PID controller

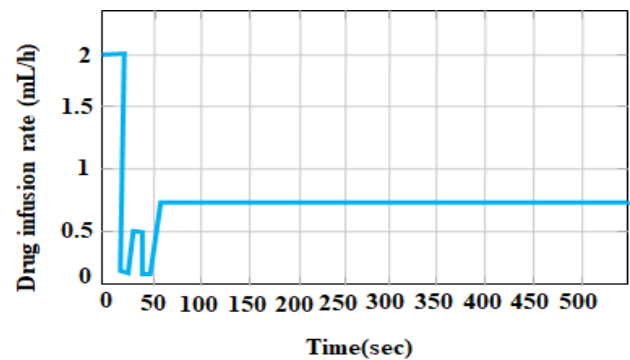


Figure 11. Control signal corresponding to the PDO-PID controller

Figure 12 demonstrates the performance of the developed controller with MPC. Additionally, it should be mentioned that the system always reacts more quickly than other controllers. This control strategy is suitable for various patients due to notable advancements in system responsiveness. While the MPC demonstrates a faster rise time and initially reaches the target output more quickly, the PDO-PID controller shows better long-term stability and reduced overshoot. The PDO-PID approach offers a smoother and more gradual transition, minimizing aggressive control actions and thus ensuring safer and more sustainable drug delivery, making it particularly suitable for sensitive physiological systems such as blood pressure regulation in post-operative patients. Figure 13 presents a comparative analysis between ABC-PID [21] and PDO-PID, based on settling time and peak time. From the analysis, PDO-PID is a slightly more efficient controller due to its lower settling time (1.05) while maintaining the lower peak time (0.203) as ABC-PID, which stabilizes the system slightly faster.

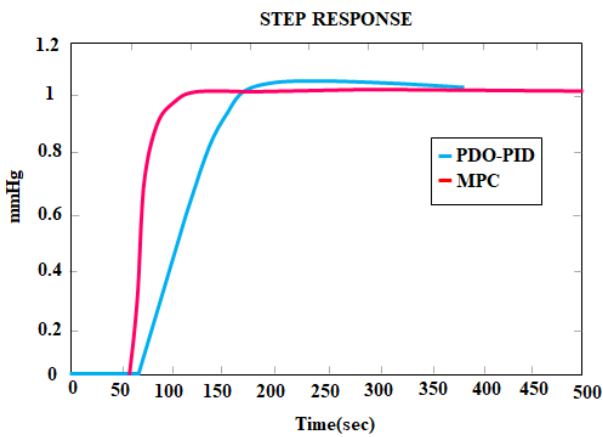


Figure 12. Step response (MAP) for controllers

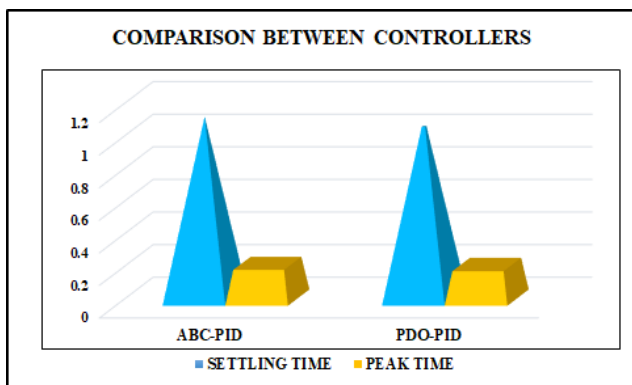


Figure 13. Analysis among controllers

Table 2 provides a performance comparison between Genetic Algorithm (GA)-based Model Predictive Control (MPC) [22-25] and the developed controller according to Integral Squared Error (ISE), Integral Absolute Error (IAE), Mean Squared Error (MSE), and Execution time. PDO-PID outperforms GA-based MPC by showing lower absolute error, ensuring that PDO-PID provides a more accurate and stable response. The developed controller consistently performs better across all performance metrics compared to GA-based MPC.

Table 2. Performance analysis among controllers

Control Approaches	GA based MPC	PDO-PID
IAE	4.42	3.87
ISE	2.10	2.01
MSE	0.011	0.01
Execution time	66.9531	63.613

An analysis of the transient response between the ABC-PID [22] and the PDO-PID controller is represented in Figure 14. The ABC-PID has a rise time of 0.0985, whereas PDO-PID has a significantly lower rise time of 0.051, which suggests that PDO-PID responds faster to changes in input and reaches the desired state more quickly. The PDO-PID also exhibits lower overshoot (0.1021), meaning it introduces fewer fluctuations and maintains better system stability. A comparative analysis of steady-state error across three different control approaches, like Grey Wolf Optimizer (GWO), Salp Swarm Algorithm (SSA), and the proposed method, is revealed in Table 3. It is a critical metric in control systems, particularly in blood pressure management, as it determines the accuracy of the system in sustaining the desired pressure level. The proposed method outperforms SSA and GWO in terms of steady-state error, particularly in normal and insensitive cases, indicating a more reliable and precise blood pressure regulation system.

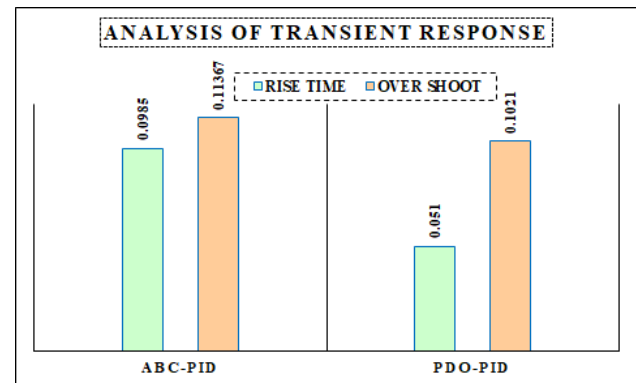


Figure 14. Comparison of transient response

Table 3. Comparison among algorithms

Cases	Error steady state(mmHg)		
	SSA [24]	GWO [25]	Proposed
Sensitive	2.58×10^{-5}	7.492×10^{-5}	2.91×10^{-5}
Normal	2.61×10^{-5}	3.838×10^{-5}	2.23×10^{-5}
Insensitive	0.00044	0.000689	0.00035

4. Conclusion

This research work proposes a novel optimized PID controller for blood pressure management. The PID controller decides the amount of SNR drug rate that is delivered to the patient, ensuring the BP is managed properly. By tuning the parameters of the PID controller, the PDO enhances the performance of the PID controller with less settling time and overshoot. By the injection pump's physical constraints, the MAP stabilizes at about 80 mm Hg after bringing the blood pressure down to a normal control level. According to the results, PDO-based PID performs better than the PID

controller with the control signal's delay and limit. The proposed research guarantees that the MAP remains at its predefined rate of 100 mmHg during surgical procedures, post-surgery recuperation, or anaesthesia administration by precisely administering the recommended amount of the SNP medicine. By calculating the SNP infusion rate, the simulation results have validated that a PID controller with PDO is helpful in controlling blood pressure. This method provided much improved performance than other approaches, mainly to cover an extensive range of patients.

Ethical issue

The authors are aware of and comply with best practices in publication ethics, specifically with regard to authorship (avoidance of guest authorship), dual submission, manipulation of figures, competing interests, and compliance with policies on research ethics. The authors adhere to publication requirements that the submitted work is original and has not been published elsewhere.

Data availability statement

Datasets analyzed during the current study are available and can be provided upon a reasonable request from the corresponding author.

Conflict of interest

The authors declare no potential conflict of interest.

References

- [1] T. E. Baum, E. Adam, C. S. Guay, G. Schamberg, M. Kazemi, T. Heldt, and E. N. Brown, "Dynamic Estimation of Cardiovascular State From Arterial Blood Pressure Recordings," in *IEEE Transactions on Biomedical Engineering*, vol. 71, no. 11, pp. 3146-3159, 2024. DOI: <https://doi.org/10.1109/TBME.2024.3408808>.
- [2] M. Liaqat, M. G. Khan, M. R. Fazal, Y. Ghadi and M. Adnan, "Multi-Criteria Storage Selection Model for Grid-Connected Photovoltaics Systems," in *IEEE Access*, vol. 9, pp. 115506-115522, 2021. DOI: <https://doi.org/10.1109/ACCESS.2021.3105592>
- [3] S. Chen, T. Rehemani, C. Li, X. Wu, H. Lin, Z. Lin, X. Liang, H. Li, and J. Zhang, "Hypertension Monitoring by a Real Time Management System for Patients in Community and Its Data Mining by Vector Autoregressive Model," in *IEEE Access*, vol. 11, pp. 12607-12622, 2023. DOI: <https://doi.org/10.1109/ACCESS.2023.3240084>.
- [4] M. A. Sultan and W. Saadeh, "Continuous Patient-Independent Estimation of Respiratory Rate and Blood Pressure Using Robust Spectro-Temporal Features Derived From Photoplethysmogram Only," in *IEEE Open Journal of Engineering in Medicine and Biology*, vol. 5, pp. 637-649, 2024. DOI: <https://doi.org/10.1109/OJEMB.2023.3329728>.
- [5] Q. Lin, T. Li, P. M. Shakeel, and R. D. J. Samuel, "Advanced artificial intelligence in heart rate and blood pressure monitoring for stress management," *Journal of Ambient Intelligence and Humanized Computing*, vol. 12, pp.3329-3340, 2021. DOI: <https://doi.org/10.1007/s12652-024-04916-6>.
- [6] J. Kitt, A. Frost, J. Mollison, K. L. Tucker, K. Suriano, Y. Kenworthy, A. McCourt, W. Woodward, C. Tan, W. Lapidaire, and R. Mills, "Postpartum blood pressure self-management following hypertensive pregnancy: protocol of the Physician Optimised Post-partum Hypertension Treatment (POP-HT) trial," *BMJ open*, vol. 12, no. 2, pp.e051180, 2022. DOI: <https://doi.org/10.1136/bmjopen-2021-051180>.
- [7] S. Tasoujian "Linear Parameter Varying Control of Uncertain Time-Delay Systems with Applications to Automated Blood Pressure Regulation," (2020).
- [8] J. G. Wang, Y. Li, Y. C. Chia, H. M. Cheng, H. V. Minh, S. Siddique, G. P. Sogunuru, J. C. Tay, B. W. Teo, K. Tsoi, and Y. Turana, "Telemedicine in the management of hypertension: evolving technological platforms for blood pressure telemonitoring," *The Journal of Clinical Hypertension*, vol. 23, no. 3, pp. 435-439, 2021. DOI: <https://doi.org/10.1111/jch.14194>.
- [9] E. C. Sandset, C. S. Anderson, P. M. Bath, H. Christensen, U. Fischer, D. Gąsecki, A. Lal, L. S. Manning, S. Sacco, T. Steiner, and G. Tsivgoulis, "European Stroke Organisation (ESO) guidelines on blood pressure management in acute ischaemic stroke and intracerebral haemorrhage," *European stroke journal*, vol. 6, no. 2, 2021. DOI: <https://doi.org/10.1177/23969873211012133>.
- [10] T. Panula, J. P. Sirkiä, D. Wong, and M. Kaisti "Advances in non-invasive blood pressure measurement techniques," *IEEE Reviews in Biomedical Engineering*, vol. 16, pp. 424-438, 2022. DOI: <https://doi.org/10.1109/RBME.2022.3141877>.
- [11] B. Citoni, I. Figliuzzi, V. Presta, M. Volpe, and G. Tocci "Home blood pressure and telemedicine: a modern approach for managing hypertension during and after COVID-19 pandemic," *High Blood Pressure & Cardiovascular Prevention*, vol. 29, no. 1, pp. 1-14, 2022. DOI: <https://doi.org/10.1007/s40292-021-00492-4>.
- [12] P. Schoettker, J. Degott, G. Hofmann, M. Proença, G. Bonnier, A. Lemkaddem, M. Lemay, R. Schorer, U. Christen, J. F. Knebel, and A. Wuerzner, "Blood pressure measurements with the OptiBP smartphone app validated against reference auscultatory measurements," *Scientific Reports*, vol. 10, no. 1, pp. 17827, 2020. DOI: <https://doi.org/10.1038/s41598-020-74955-4>.
- [13] T. Gazit, M. Gutman, and A. L. Beatty "Assessment of hypertension control among adults participating in a mobile technology blood pressure self-management program," *JAMA Network Open*, vol. 4, no. 10, pp. e2127008-e2127008, 2021. DOI: [10.1001/jamanetworkopen.2021.27008](https://doi.org/10.1001/jamanetworkopen.2021.27008).
- [14] V. T. Mai, K. A. Alattas, Y. Bouteraa, E. Ghaderpour, and A. Mohammadzadeh, "Personalized Blood Pressure Control by Machine Learning for Remote Patient Monitoring," *IEEE Access*, vol. 12, pp.83994-84004, 2024. DOI: <https://doi.org/10.1109/ACCESS.2024.3413572>.
- [15] T. Fujiwara, S. Hoshida, H. Kanegae, and K. Kario, "Cardiovascular event risks associated with masked nocturnal hypertension defined by home blood pressure monitoring in the J-HOP nocturnal blood pressure study," *Hypertension*, vol. 76, no. 1, pp. 259-266, 2020. DOI: <https://doi.org/10.1161/HYPERTENSIONAHA.120.14790>.

- [16] J. Leitner, P. H. Chiang, and S. Dey, "Personalized blood pressure estimation using photoplethysmography: A transfer learning approach," *IEEE Journal of Biomedical and Health Informatics*, vol. 26, no. 1, pp. 218-228, 2021. DOI: <https://doi.org/10.1109/JBHI.2021.3085526>.
- [17] N. Pachauri, and G. B. K, "Automatic drug infusion control based on metaheuristic H2 optimal theory for regulating the mean arterial blood pressure," *Asia-Pacific Journal of Chemical Engineering*, vol. 16, no. 4, pp. e2654, 2021. DOI: <https://doi.org/10.1002/apj.2654>.
- [18] B. Aubouin-Pairault, M. Fiacchini, and T. Dang, "Automated multi-drugs administration during total intravenous anesthesia using multi-model predictive control," *arXiv preprint arXiv:2309.08229*, 2023. DOI: <https://doi.org/10.48550/arXiv.2309.08229>
- [19] K. Saravanakumar, and J. Samson Isaac. "IMO-PSO FO-PID controller based insulin infusion system for type 1 diabetes patients during post-operation condition," *Measurement: Sensors*, vol. 33, pp. 101172, 2024. DOI: <https://doi.org/10.1016/j.measen.2024.101172>.
- [20] M. R. Ahmadpour, H. Ghadiri, and S. R. Hajian, "Model predictive control optimisation using the metaheuristic optimisation for blood pressure control," *IET Systems Biology*, vol. 15, no. 2, pp. 41-52, 2021. DOI: <https://doi.org/10.1049/syb2.12012>.
- [21] V. Dubey, H. Goud, P. C. Sharma, and S. Anjana, "Designing of intelligent PID controller for cardiac pacemaker using artificial bee colony algorithm," *Systems Science & Control Engineering*, vol. 12, no. 1, pp. 2347891, 2024. DOI: <https://doi.org/10.1080/21642583.2024.2347891>.
- [22] V. Dubey, H. Goud, P. C. Sharma, and S. Anjana, "Designing of intelligent PID controller for cardiac pacemaker using artificial bee colony algorithm," *Systems Science & Control Engineering*, vol.12, no. 1, pp. 2347891, 2024. DOI: <https://doi.org/10.1080/21642583.2024.2347891>.
- [23] M. R. Ahmadpour, H. Ghadiri, and S. R. Hajian, "Model predictive control optimisation using the metaheuristic optimisation for blood pressure control," *IET Systems Biology*, vol. 15, no. 2, pp. 41-52, 2021. DOI: <https://doi.org/10.1049/syb2.12012>.
- [24] R. Haamed, "Controlling of Mean Arterial Pressure by Modified PI-ID Controller Based on Two Optimization Algorithms," 2020. DOI: 10.5815/ijmecs.2020.04.04.
- [25] R. Haamed, and E. Hameed, "Controlling the mean arterial pressure by modified model reference adaptive controller based on two optimization algorithms," *Applied Computer Science*, vol. 16, no. 2, 2020. DOI: <http://dx.doi.org/10.23743/acs-2020-12>.



This article is an open-access article distributed under the terms and conditions of the Creative Commons Attribution (CC BY) license (<https://creativecommons.org/licenses/by/4.0/>).